JOURNAL OF MATERIALS SCIENCE 25 (1990) 4535-4540

The use of foil metallurgy processing to achieve ultrafine grained Mg–9Li laminates and Mg–9Li–5B_4C particulate composites

G. GONZÁLEZ-DONCEL*, J. WOLFENSTINE†, P. METENIER, O. A. RUANO*, O. D. SHERBY
Department of Materials Science and Engineering, Stanford University, Stanford, California 94305, USA

A foil metallurgy processing technique has been developed to prepare fine-grained laminates based on a two-phase Mg–9Li alloy and fine-grained particulate composites based on hard B_4C powders embedded in the two-phase Mg–9Li alloy. The processing steps involve principally cold-rolling and low-temperature recovery processing for preparation of foils, and low-temperature press-bonding for preparation of laminates and composites. In this manner, contamination of the highly reactive alloy is minimized. Good tensile strength and ductility were achieved at room temperature with specific stiffness values of about 3.1×10^6 m^3. Both the fine-grained laminates and the particulate composite are superplastic at 200° C, exhibiting a strain-rate-sensitivity exponent, m, of 0.5.

1. Introduction

Magnesium–lithium alloys have potential for use in aerospace applications because they are exceptionally light and their specific stiffness is high [1]. The purpose of this paper is to describe a thermo-mechanical processing method, utilizing foil metallurgy, to make fine-grained laminates of a two-phase Mg–Li alloy. The method involves processing steps which include extensive cold-rolling of a casting with intermediate annealing steps at low homologous temperatures (about 0.5 T_m, where T_m is the absolute melting temperature). In this manner, oxidation and corrosion reactions are minimized, an important consideration in highly reactive Mg–Li alloys. Furthermore, it will be shown that a particulate composite of the two-phase Mg–Li alloy containing elastically stiff B_4C particles can be readily prepared at low temperatures by press-bonding the fine-grained Mg–Li foils with alternating layers of B_4C powders. An added benefit of the fine grains in the laminates and particulate composite is that superplastic behaviour can be expected at intermediate temperatures. The foil metallurgy processing to be described can be potentially more attractive than powder metallurgy processing because of a decreasing tendency for contamination due to the low surface to volume ratio in the foils.

2. Experimental procedure

2.1. Preparation of fine-grained Mg–9Li laminates

Mg–9 wt % Li cylindrical castings were supplied by the Naval Surface Weapons Center, Silver Springs, Maryland, USA. The castings consisted of two phases; α, an hexagonal-close-packed structure, and β, a body-centred-cubic structure. The proportion of each phase at room temperature is 29% α and 71% β. The purpose of selecting a two-phase Mg–Li alloy was to achieve a stable fine grain size, each phase preventing the other from growing. The microstructure of the coarse-grained as-cast material is shown in Fig. 1. The α phase is elongated and dispersed within the β matrix. The linear intercept grain size of the beta phase in the as-cast structure is of the order of 50 to 100 μm. The etchant used for all metallographic examinations was a 10% HCl, 90% ethanol mixture.

In order to refine the grains, the as-cast material was cut into plates (thickness between 10 and 15 mm) and given the thermo-mechanical processing procedure shown in Fig. 2. Typically, four cold-rolling and annealing steps were used, with a total reduction of about 170 : 1, leading to foils about 0.2 mm thick. The purpose of the annealing steps (130° C for 0.5 h in air) was to allow recovery to occur, so that additional cold-rolling could be performed without the formation of edge-cracks.

The foils were cut into 25 mm × 35 mm rectangles and stacked together, where the number of foils stacked varied between 90 and 330. No surface treatment was given to the foils. The stacked foils were then press-bonded at temperatures between 180 and 230° C (0.5 to 0.6 T_m) for about 0.5 h in air, with loads between 0.4 and 0.9 MN. The stacked foils were typically given a reduction of between 3 and 15 to 1.

* *Present address*: Centro Nacional de Investigaciones Metalúrgicas, Av. de Gregorio del Amo 8, 28040 Madrid, Spain.
† *Present address*: Department of Mechanical Engineering, University of California, Irvine, CA92717, USA.

0022–2461/90 $03.00 + .12

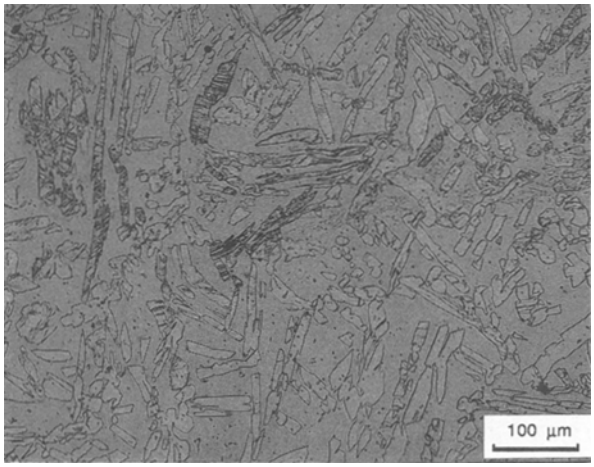

Figure 1 Microstructure of the two-phase as-cast Mg–9Li alloy. The α phase is elongated and dispersed within the β matrix.

2.2. Preparation of a fine-grained Mg–9Li–5B_4C particulate composite

The B_4C powders were obtained from the Naval Surface Weapons Center, Silver Springs, Maryland, USA. The powders have a blocky shape, with sizes typically less than 20 μm. The as-received B_4C particles were soaked in a 5% HCl, 2% HF, and 93% ethanol solution for 1 h to remove any surface contamination. After soaking, they were filtered with ethanol and dried. The B_4C particles were then suspended in an ethanol solution to form a paste. The paste was painted on to one side of the Mg–9Li foils. The amount of B_4C was determined by the change in weight of the foils before and after application of the B_4C powder. The foils were dried at room temperature and then stacked together and press-bonded. Similar conditions to those previously described for the preparation of the Mg–9Li laminates were used, resulting in an Mg–9Li–5B_4C (5 = wt % B_4C) particulate composite. The amount of reduction during press-bonding was about 5 : 1.

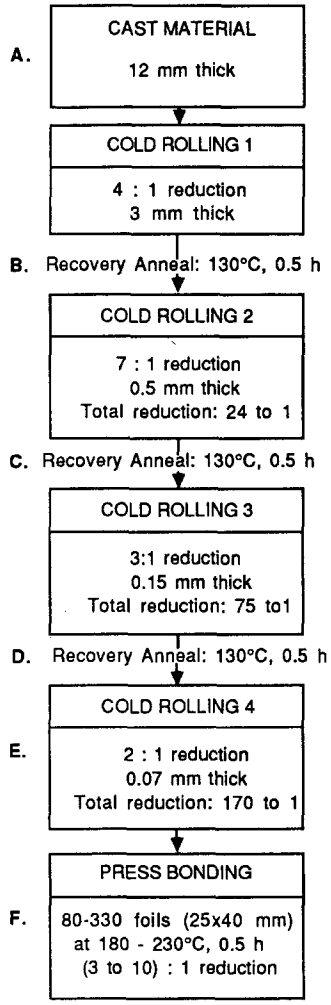

Figure 2 Flow chart illustrating the method to prepare Mg–9Li foils from a casting by cold-rolling and annealing steps.

2.3. Mechanical testing and density measurements

Tensile specimens of 10 mm effective gauge length were machined from the as-cast, laminate, and particulate composite materials. Room-temperature stress–strain curves for all three materials were determined at a constant true strain rate using an Instron machine. Elevated temperature (200° C, $T = 0.55\ T_m$) change-in-strain-rate tests were performed to determine the strain-rate-sensitivity exponents [2]. Strain rates varied between 4×10^{-5} and $3 \times 10^{-2}\ sec^{-1}$. Elongation-to-failure tests at constant true strain rates were conducted to determine the tensile ductility of all three materials. The temperature gradient along the gauge length was ± 2° C for all strain-rate-change and elongation-to-failure tests. The densities of the as-cast, laminate, and particulate composite were measured using the two-fluid method, with air and absolute methanol as fluids.

3. Results and discussion

The thermo-mechanical processing steps described above led to the preparation of fine-grained Mg–9Li laminates. This success centred on a series of cold-rolling and annealing steps, followed by press-bonding of the resulting thin foils at low homologous temperatures. The microstructures after each of the four cold-rolling and annealing sequences are shown in Fig. 3. The photomicrographs reveal the evolution of a directionally worked structure. The banded structure is seen to become narrower after each successive rolling and annealing step. The average band spacing after the initial 4 : 1 reduction is about 10 μm, after the 24 : 1 reduction it is about 3 μm, after the 75 : 1 reduction it is about 1 μm, and after the final 170 : 1 reduction it is about 0.5 μm. No microstructural evidence of recrystallization was noted after annealing at 130° C, 0.5 h. Other rolling procedures wherein the as-cast material was given reductions of 4 : 1, 15 : 1, 50 : 1, and 75 : 1 and then heated to 180° C for 0.5 h, also showed no microstructural evidence for recrystallization. If the same foils were heated at 250° C for 0.5 h, however, complete recrystallization (equiaxed grains) appeared, but only in foils with reductions of greater than 75 : 1.

The final step of press-bonding was used as the method of consolidation, as well as for controlling the final grain size. It was discovered that recrystallization was enhanced when simultaneous deformation took place (dynamic recrystallization). For example, recrystallization occurred at pressing temperatures as low as

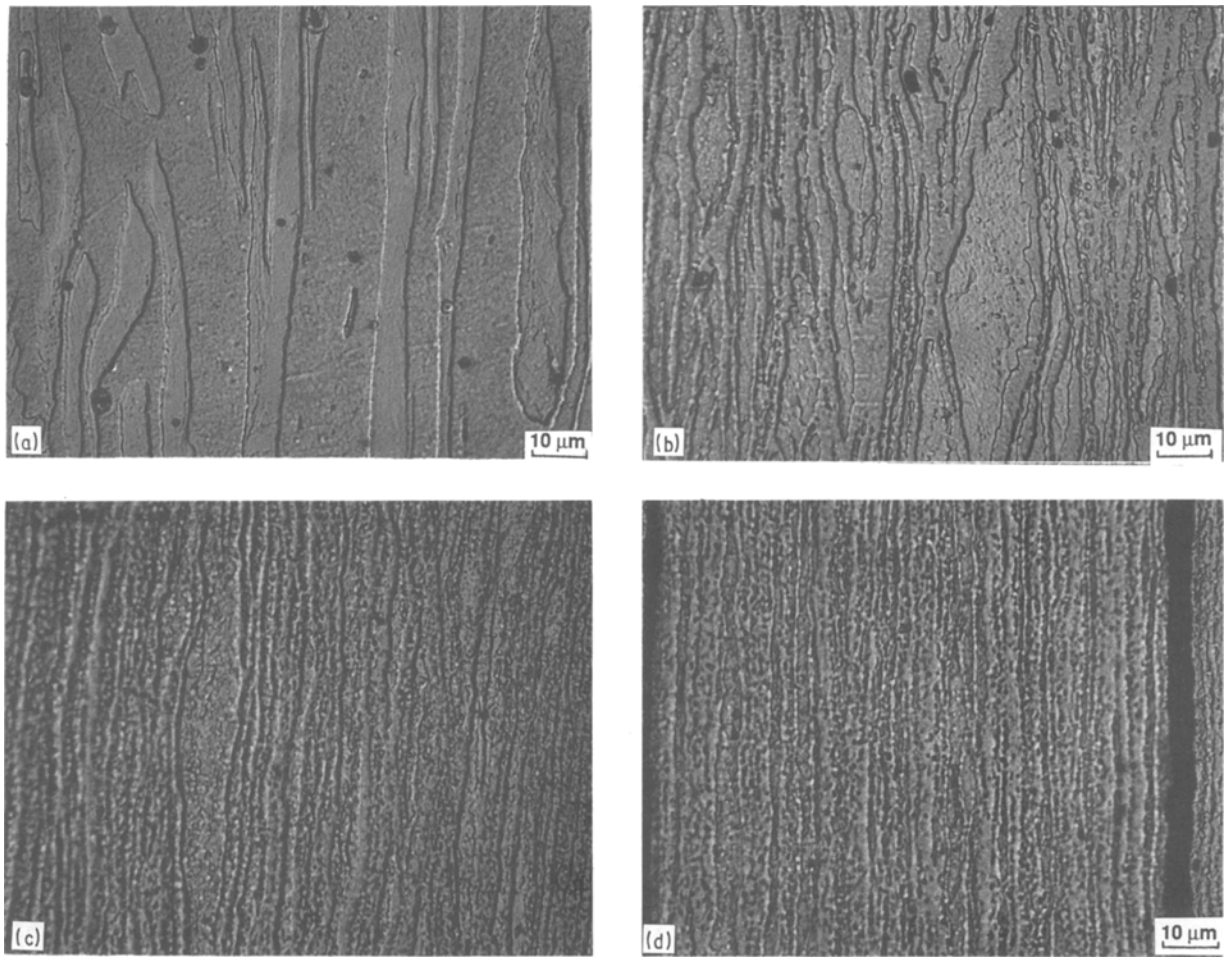

Figure 3 Microstructure of the Mg–9Li as-cast material after each cold-rolling and annealing step, shown in Fig. 2, illustrating the evolution of a worked structure (a) after 4 : 1 reduction, (b) after 24 : 1 reduction, (c) after 75 : 1 reduction, (d) after 170 : 1 reduction.

180° C. The grain size of the pressed laminates, however, was primarily a function of the amount of prior cold-working for foils given the same annealing treatment. The greater the amount of total cold-rolling, the smaller the final grain size. An example of this trend is shown in Fig. 4. The microstructure of a laminate, consisting of foils reduced 60 : 1, press-bonded at about 200° C, is shown in Fig. 4a. A linear intercept grain size, $\bar{L}$, of 12 μm is observed. On the other hand, a laminate, consisting of foils reduced 170 : 1, also press-bonded at 200° C, results in a linear intercept grain size of 3 μm. The microstructure of this laminate is shown in Fig. 4b. Cold reductions between 60 : 1 and 170 : 1 lead to linear intercept grain sizes between 3 and 12 μm.

The presence of a dark layer between the Mg–9Li layers was often observed (Fig. 4a). Auger electron spectroscopy revealed that the dark layer between the foils is Li_2O. A comparison of the densities between the laminate ($\rho = 1.54\,Mg\,m^{-3}$) and the as-cast material ($\rho = 1.50\,Mg\,m^{-3}$) confirmed that the dark layer between the foils is not porosity. The fraction of Li_2O is between 2 and 5 vol %. The Li_2O regions originate from the oxide layers on both surfaces of the

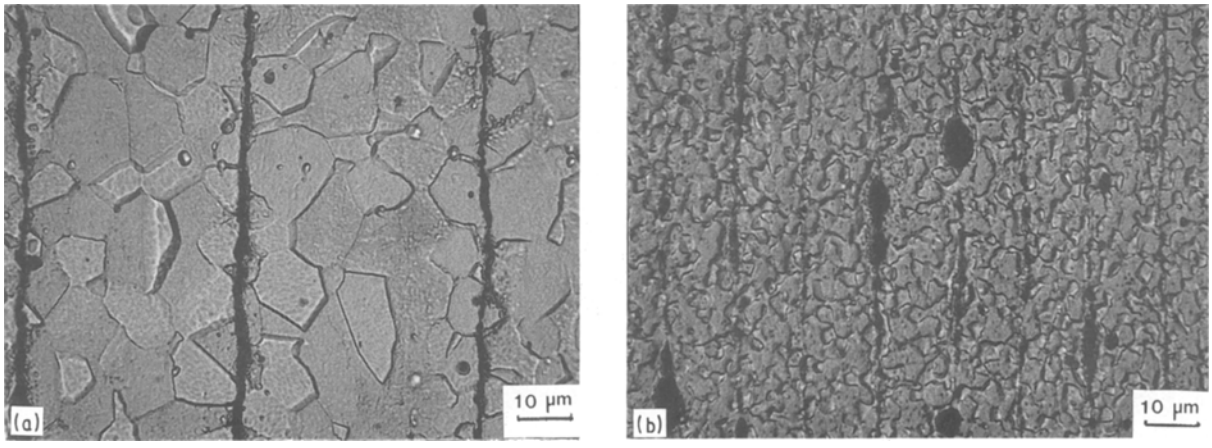

Figure 4 Microstructure of Mg–9Li laminates press-bonded at 200° C. (a) Foils reduced 60 : 1; (b) foils reduced 170 : 1.

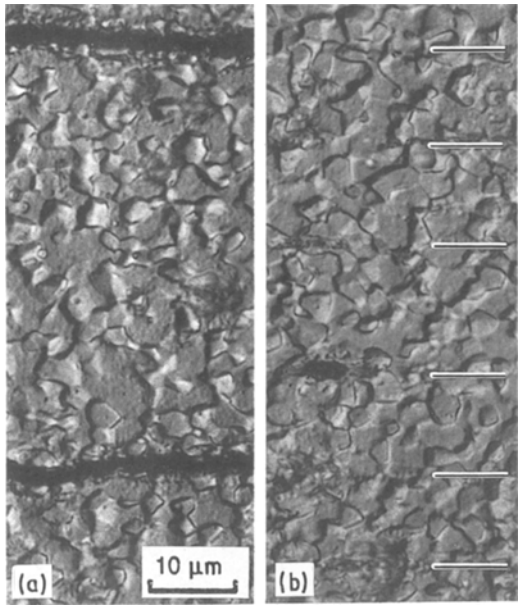

Figure 5 Microstructure of Mg–9Li laminate press-bonded at 200° C. (a) Reduction during press-bonding was 3 : 1. (b) Reduction during press-bonding was 15 : 1. Marks on Fig. 5b indicate the interface between foils.

as-rolled foils prior to press-bonding. The amount of Li_2O material is a strong function of the degree of deformation during press-bonding. Fig. 5 compares the microstructure of a laminate, consisting of foils cold reduced 150 : 1, as influenced by plastic deformation during press-bonding ($T \approx 200°$ C). Fig. 5a shows a continuous Li_2O layer is between the foils when the reduction during press-bonding is about 3 : 1. In contrast, Fig. 5b shows only discrete and discontinuous Li_2O when the reduction during press-bonding is about 15 : 1. In both cases, the final grain size is the same, $\bar{L} \approx 3\,\mu$m, confirming the general observation that the principal factor influencing the final grain size is the amount of cold work induced in the foils. The fine grains present can enhance the bonding of foils during pressing because of the many high-angle boundaries present at the interface. The high-angle grain boundaries permit rapid removal of vacancies and foreign atoms from the interface and therefore better bonding between layers is obtained [3].

TABLE I Room-temperature properties

	Mg–9Li		Mg–9Li–5B_4C
	As-cast	Laminate	Particulate composite
E (GPa)	45.4	47.7	49.0
ρ (Mg m^{-3})	1.50	1.54	1.58
E/ρ (10^6 m^3)	3.09	3.15	3.16
σ_y (MPa)	110	133	162
e_f (%)	55	22	13

Fig. 6 illustrates the microstructure of a 170 layer Mg–9Li–5B_4C particulate composite press-bonded at 200° C. A fine grain size of $\bar{L} \approx 2\,\mu$m is observed in the Mg–9Li matrix, with a uniform distribution of B_4C. The large reduction in thickness during the cold-rolling steps of the Mg–9Li foils resulted in the small final matrix grain size. As with the Mg–9Li laminate, Li_2O is observed at certain locations along the interface between the foils in the Mg–9Li–5B_4C composite. The random distribution of boron carbide particles is a result of the relatively thin foils used, the presence of a small volume fraction of B_4C, and the ease of flow of the fine-grained Mg–9Li foils around the particles during press-bonding.

The Mg–9Li alloy containing B_4C particles prepared by the foil metallurgy technique is similar to the approach used by Ghosh *et al.* [4] in fabricating SiC/Al composites. Ghosh *et al.* added SiC carbide whiskers between foils of a superplastic aluminium alloy followed by press-bonding at elevated temperature. The SiC/Al composite was evaluated for its mechanical properties at room temperature and compared with a similar composite prepared by powder metallurgy. It was shown that the foil and powder-processed materials exhibited improved modulus values over that for the aluminium alloy. In addition, the composite prepared by foil metallurgy processing exhibited higher tensile ductility at room temperature than the composite prepared by powder metallurgy processing.

The room-temperature static elastic modulus (E), density (ρ), specific stiffness (E/ρ), yield strength (σ_y), and tensile ductility (e_f), for the as-cast, laminate, and particulate composite materials are listed in Table I. This table shows that the room-temperature yield strength of the Mg–9Li–5B_4C composite is greater

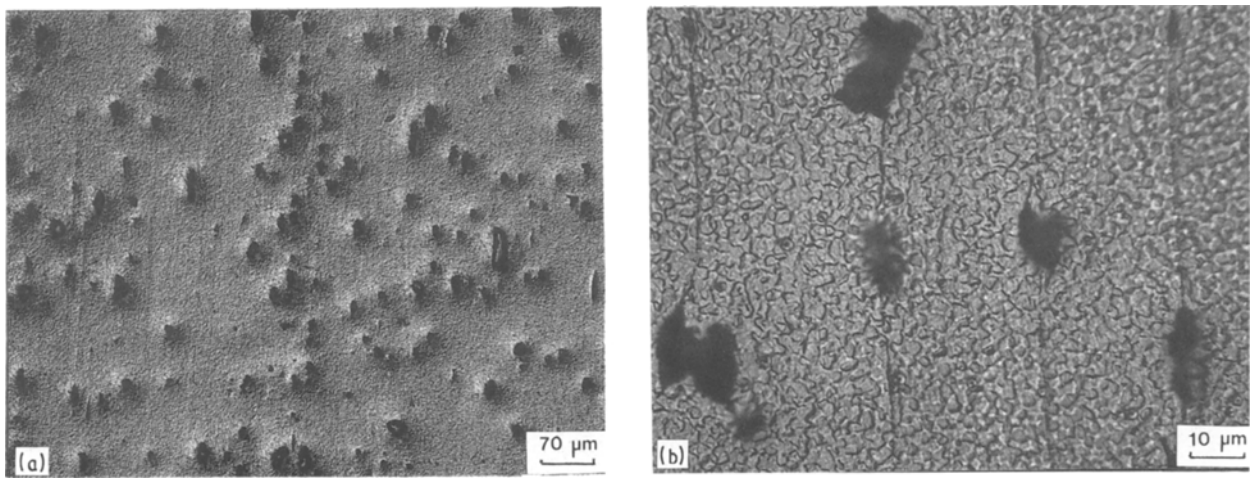

Figure 6 Microstructure of the press-bonded 170 layer Mg–9Li–5B_4C particulate composite. (a) Low magnification showing a uniform distribution of B_4C particles, (b) high-magnification showing the fine grain size of the Mg–9Li matrix.

than that for the Mg–9Li laminate which, in turn, is greater than that for the Mg–9Li as-cast material. Good tensile ductility was achieved for all three materials; 50% elongation was obtained in the as-cast material and 13% elongation for the Mg–9Li–5B_4C particulate composite. The higher yield strength of the particulate composite and the laminate compared to the as-cast material is a result of their finer grain sizes. The large grain size of the as-cast material, however, allows for greater strain hardening than in the fine-grained laminate and particulate composite and consequently, a higher tensile ductility is observed for the as-cast material. The Young's modulus of the laminate and the particulate composite is higher than that for the as-cast material. This can be attributed to the presence of the Li_2O and B_4C compounds. The specific stiffness values for the as-cast, laminate, and the particulate composite are, 3.09×10^6, 3.15×10^6, and 3.16×10^6 m^3, respectively. These values are higher than for most commercial aluminium and titanium alloys ($E/\rho \approx 2.6 \times 10^6$ m^3) [5].

The fine grain size developed in the Mg–9Li materials by foil metallurgy processing would suggest that superplastic properties are achievable at elevated temperature. Strain-rate-change tests and elongation-to-failure tests were conducted at 200° C to evaluate the superplastic behaviour of the laminate and the particulate composite. Fig. 7 shows the strain-rate-change tests for the as-cast Mg–9Li, Mg–9Li laminate ($\bar{L}_{initial} \approx 3\,\mu m$), and Mg–9Li–5$B_4C$ particulate composite ($\bar{L}_{initial} \approx 2\,\mu m$). The figure is a plot of the logarithm of the flow stress against the logarithm of the true strain rate. The data can be analysed by the following relation, $\sigma = k\dot{\varepsilon}^m$, where σ is the steady-state flow stress, k is a constant (which is function of both temperature and microstructure), $\dot{\varepsilon}$ is the true strain rate, and m is the strain-rate-sensitivity exponent. The slope of the curves is the strain-rate-sensitivity exponent. For the coarse grained as-cast material, the m value is about 0.2 over the entire range of strain rates. This value is typical for a coarse-grained material, where a diffusion-controlled dislocation process dominates deformation [6, 7]. The fine-grained laminate and particulate composite exhibit high m values (≈ 0.5) at low strain rates. A value of m equal to 0.5 is indicative that the rate-controlling deformation mechanism is grain-boundary sliding [8, 9]. In the grain-boundary sliding region, superplastic deformation is expected, and the flow stress is a strong function of grain size, decreasing with a decrease in grain size [8, 10]. Thus, the finer grain size of the particulate composite compared to the laminate explains why the flow stress of the particulate composite is lower than that for the laminate. In turn, both the laminate and the particulate composite are weaker than the coarse-grained cast Mg–9Li alloy. In the high strain-rate range, the fine-grained laminate and particulate composite exhibit low m values as slip processes become rate controlling. As expected, the fine-grained materials are seen to be slightly stronger than the coarse-grained as-cast material in this strain-rate range.

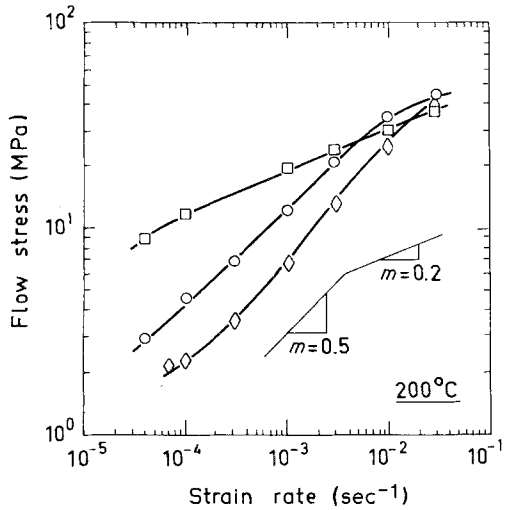

Figure 7 Flow stress–strain rate diagram for the (□) as-cast Mg–9Li, $L = 100\,\mu m$, (○) Mg–9Li laminate, $L = 3\,\mu m$, and (◇) Mg–9Li–5B_4C particulate composite, $L = 2\,\mu m$, at 200° C.

Elongation-to-failure tests performed at a true strain rate of 10^{-3} sec^{-1} and 200° C exhibited large elongations for the laminate (455%) and particulate composite (355%). The as-cast material exhibited only 70% elongation. These results are expected based on the strain-rate-change tests.

4. Conclusions

1. A fine-grained Mg–9Li laminate alloy can be made by a thermo-mechanical process based on low-temperature press-bonding of cold-rolled and annealed foils. Using a similar process, a particulate composite of Mg–9Li containing 5 wt % B_4C can be prepared.

2. The final grain size of the laminates and the particulate composite is a strong function of the total amount of reduction in foil thickness during cold-rolling. The greater the amount of cold-working, the smaller the final grain size.

3. Room-temperature properties reveal that good tensile ductility is achieved for the laminate and particulate composite with yield strengths about 50% higher than in the as-cast condition. The specific stiffness of the Mg–9Li–5B_4C particulate composite is 3.16×10^6 m^3, about 22% above that measured for commercial aluminium and titanium alloys.

4. The fine-grained laminates and the particulate composite exhibit superplastic behaviour at elevated temperature.

5. Foil metallurgy processing of Mg–9Li alloys for achieving fine-grained structures is potentially more attractive than powder metallurgy processing because contamination is reduced due to the low surface to volume ratio in the foils.

Acknowledgements

The US Office of Naval Research provided financial support for this programme under contract N-0014-82-K-0314. The authors gratefully acknowledge the technical advice and assistance of Dr George Yoder, Materials Branch, ONR, Messrs A. P. Divecha and S. Karmarkar, Naval Surface Weapons Center, Silver Springs, Maryland, who provided the Mg–9Li castings and B_4C powders used in this investigation, and Dr Jeffrey Wadsworth, Lockheed Palo Alto Research Laboratory, who provided the room-temperature

mechanical tests and Auger electron spectroscopy results.

References

1. R. K. WYSS, "Advances in Magnesium Alloys and Composites", edited by H. Paris and W. H. Hunt (The Minerals and Metals and Materials Society, Warrendale, Pennsylvania, 1988) p. 25.
2. B. WALSER and O. D. SHERBY, *Metall. Trans.* **10A** (1979) 1461.
3. O. D. SHERBY, B. WALSER, C. M. YOUNG and E. M. CADY, *Scripta. Metall.* **13** (1979) 914.
4. A. K. GHOSH, C. H. HAMILTON and N. E. PATON, *US Pat.* 4469757, 4 September, 1984.
5. R. T. WHALEN, G. GONZÁLEZ-DONCEL, S. L. ROBINSON and O. D. SHERBY, *Scripta Metall.* **23** (1989) 137.
6. O. D. SHERBY and P. M. BURKE, *Prog. Mater. Sci.* **13** (1967) 25.
7. J. WEERTMAN, *Trans. ASM* **61** (1968) 681.
8. O. D. SHERBY and J. WADSWORTH, in "Deformation Processing and Structure", edited by G. Krauss (American Society for Metals, Metals Park, Ohio, 1982) p. 355.
9. J. W. EDINGTON, K. N. MELTON and C. P. CUTLER, *Prog. Mater. Sci.* **21** (1976) 61.
10. A. K. MUKHERJEE, *Ann. Rev. Mater. Sci.* **13** (1979) 53.

Received 31 May
and accepted 23 October 1989